Quantum Mechanical Investigation of the Influence of the Local Environment on the Vibrational Properties of Hydrogenated Si(111)

M. F. Juarez,[†] E. M. Patrito,[‡] and P. Paredes-Olivera*[,†]

Unidad de Matemática y Física, and Departamento de Fisicoquímica, Instituto de Investigaciones en Fisicoquímica de Córdoba (INFIQC), Facultad de Ciencias Químicas, Universidad Nacional de Córdoba, Ciudad Universitaria, 5000 Córdoba, Argentina

Received: September 11, 2008; Revised Manuscript Received: November 6, 2008

Periodic density functional calculations were performed to investigate the vibrational properties of hydrogenated and grafted Si(111) surfaces as a function of surface coverage and subsurface oxidation. Surfaces terminated with $-CH_3$, $-CCH$, and $-Cl$ groups were considered. Subsurface oxidation was taken into account by oxidizing one, two, and three silicon back bonds. The effect of anharmonicity was considered in the calculation of the stretching frequencies of the Si−H and C−H groups. The effect of the different adsorbates on the polarization of the electron density of the SiH group and on the electronic structure of the surface was investigated by means of electron density difference and density of states analyses. The Si−H stretching frequency increases with the surface coverage of $-CCH$ and $-Cl$ species, and it decreases with the increase in the surface coverage of $-CH_3$. Positive (negative) frequency shifts correlate with the increase (decrease) of electron density along the Si−H bond. The Si−H stretching frequency shows a very good correlation with the Si−H bond length for all the systems investigated. The Si−C, C−H, and Si−Cl stretching frequencies increase linearly with the surface coverage of the $-CH_3$, $-CCH$, and $-Cl$ groups. The back-bond oxidation of a SiH group produces an increase in its stretching frequency and a decrease of the stretching frequency of the surrounding unoxidized SiH groups. All the calculated frequencies show very good agreement with the experimental values.

Introduction

Vibrational spectroscopy is among the most powerful probes of fundamental processes in microelectronics. In particular, infrared (IR) absorption spectroscopy provides insight into critical aspects of silicon surface structure and reactivity through analysis of the vibrational frequencies, band intensities, and line shapes. Changes in the surface infrared spectrum upon reactive exposure can be used to extract information concerning the chemical identity, surface coverage, and dynamic properties of the surface layer.[1,2]

The Si−H stretching vibration of the Si(111)−H surface gives one of the narrowest lines observed up to now in vibrational surface spectroscopy and reflects the high quality of this surface. The close spacing of surface adsorbates has a pronounced effect on the vibrational spectrum because the motion of an individual oscillating dipole is influenced by the electric dipole field generated by the motion of its neighbors. This effect, known as dynamic dipole coupling, forces adsorbates bound to a surface to vibrate en masse instead of individually and shifts the vibrational transition to higher energy. An isolated H atom bound to a Si(111) surface would have a so-called *singleton* vibrational transition at $\sim$2080 cm^{-1}, whereas a complete, defect-free monolayer of Si−H oscillators would have a similar transition at $\sim$2085 cm^{-1}. Disordered or defective arrays would have transitions between these two extremes. Because of this, the position and structure of the vibrational transition are sensitive to the surface morphology.[3,4] Therefore, the absorption frequency allows an evaluation of the quality of the surface.

The typical IR spectrum observed for an atomically flat hydrogen-terminated Si(111) surface after removal of the native oxide exhibits two positive sharp vibrational modes assigned to the stretch (2083.7 cm^{-1}) and bend (626 cm^{-1}) modes of Si−H.[5] However, if the SiH group is within a microfacet (instead of an infinite surface), the stretching frequency decreases to 2081.3 cm^{-1}. This red shift is attributed to a reduced dynamic dipole coupling on microfacets.[6]

After exposure to chlorine gas, the Si−H modes are completely removed and two new absorbance features are observed and assigned to the stretch (586 cm^{-1}) and bend (528 cm^{-1}) modes of Si−Cl. These results indicate that on an atomically flat Si(111) surface, all the hydrogen atoms are exchanged by chlorine atoms with no etching or roughening.[7−9]

Transmission infrared spectroscopy (TIRS) has been used to investigate the surface-bound species formed in the two-step chlorination/alkylation reaction of crystalline (111)-oriented Si surfaces. The CH_3-terminated Si(111) surface exhibits distinct peaks in the C−H stretching region at approximately 2900 cm^{-1}. Peaks at 2909 and 2965 cm^{-1} are attributed to the methyl C−H symmetric and asymmetric stretching vibrations, respectively.[10]

The Si−H stretching vibration with back-bond oxidation is observed as broad bands in the higher energies; i.e., that for $(SiO_2)Si-H$ is observed at about 2200 cm^{-1} and that for $(O_3)Si-H$ at about 2250 cm^{-1}.[11−16] In a study of the kinetics of oxidation of Si(111)−H surfaces stored in humid air, it was found that the hydrogenated silicon atom having the three back bonds oxidized is kinetically stable and is the predominant species on the surface after several hours in humid air. The evidence for this is the observation of the growth of an IR absorption at 2250 cm^{-1} at the expense of the $(Si_3)Si-H$ stretch at 2084 cm^{-1}.[12]

* Corresponding author. E-mail: patricia@fcq.unc.edu.ar. Phone: 54-351-4344972.
[†] Unidad de Matemática y Física.
[‡] Departamento de Fisicoquímica.

10.1021/jp808104f CCC: $40.75
Published on Web 12/10/2008

The S−H vibrational frequency has been investigated within the harmonic approximation using both cluster and periodic slab models of the surface. Due to incomplete treatment of electron correlation, neglect of mechanical anharmonicity, and basis set truncation effects, calculated harmonic frequencies generally overestimate experimental wavenumbers. To improve the agreement between the predicted and observed frequencies, the computed harmonic frequencies are usually scaled for comparison.[17] In other cases, the calculated frequencies for the ν_s(Si−H) modes were corrected for systematic deficiencies due to anharmonic effects by substracting 102 cm^{-1}.[18]

The frequency of the Si−H stretching mode was calculated for the Si(100)-(2 × 1) surface using the cluster approximation in studies of NH_3 dissociation[18] and oxygen incorporation.[19] In the case of the Si(111)−H surface, a Si−H stretching frequency of 2056.41 cm^{-1} was calculated using the slab model of the surface.[20] Periodic density functional calculations were also used to determine the frequency shifts of deuterated versus hydrogenated Si(111) surfaces.[21] In this study, a Si−H stretching frequency of 2120 cm^{-1} was obtained.[21] Harmonic frequencies for the fully methylated Si(111) surface were calculated from density functional theory using both periodic boundary conditions and cluster models at the same level of theory.[22] The anharmonic Si−H stretching frequency was calculated on flat[23] and stepped[24] Si(111)−H surfaces using the first-principles Car−Parrinello molecular dynamics method combined with a Fourier analysis of the surface atom motions. A stretching frequency of 1965 cm^{-1} was obtained on the flat surface.[23]

In the present work, first-principles calculations based on density functional theory together with a periodic representation of the surface were carried out to investigate the vibrational properties of hydrogenated and grafted Si(111) surfaces as a function of surface coverage and subsurface oxidation. Anharmonic effects were considered in the calculation of Si−H and C−H vibrational frequencies. On the unoxidized surfaces, the shift of the Si−H stretching frequency as a function of the surface coverage of $-CH_3$, −CCH, and −Cl species correlates with the polarization of the electron density of the Si−H bond induced by the surrounding adsorbates. On the oxidized surfaces, the variation of the Si−H stretching frequency was investigated as a function of the number of Si−Si backbonds oxidized. For all the systems investigated the Si−H stretching frequency shows a very good correlation with the Si−H bond length.

Theoretical Methods and Surface Modeling

The (111) face of silicon was modeled by means of a silicon slab six layers thick. Periodic boundary conditions were applied to avoid edge effects. The dangling bonds of the bottom surface were saturated with hydrogen atoms. To ensure that there are no residual forces in the unit cell, we determined the equilibrium bulk structure of silicon, obtaining 5.48 Å for a_0, which compares very well with the experimental value of 5.43 Å.[25] The positions of all the adsorbate atoms as well as those of the four topmost Si layers were fully optimized. The unit cells employed were (1 × 1) and (2 × 2).

The calculations were performed with the CRYSTAL code which expands the crystalline orbitals in terms of a Gaussian type basis set. The following Gaussian type orbitals were used (the α exponents of the most diffuse shells are given in $bohr^{-2}$): 6-21G* basis set for Si[26] (α_{sp}= 0.123 339 2, α_d = 0.5) and 21G* for H.[26] For C, O, and Cl we used the standard 6-21G basis sets supplied by CRYSTAL. The PBE Hamiltonian was adopted.[27] The number of reciprocal lattice points (*k*-points) at which the Hamiltonian matrix was diagonalized was 36 corresponding to a shrinking factor $S = 6$. The gradient with respect to the atomic coordinates was evaluated analytically. The equilibrium atomic positions were determined using the BFGS algorithm.[28] The optimization convergence was checked on the root-mean-square and the absolute value of the largest component of both the gradients and the estimated displacements. The threshold for the maximum and the rms forces were 0.000 45 and 0.0003 au. The corresponding thresholds for the atomic displacements were 0.0075 and 0.005 au, respectively. When these four conditions were all satisfied at a time, the optimization was considered complete.

Within the harmonic approximation, the vibrational frequencies at the Γ point were calculated by diagonalizing the mass-weighted Hessian matrix, obtained by numerical differentiation of the analytical gradient with respect to the atomic coordinates.[29] The procedure adopted in this work to compute the anharmonicity of the SiH stretching was successfully employed in previous studies of the OH stretching vibration.[30−32] It consists of the following steps: (i) the SiH distance is treated as a pure normal coordinate decoupled with respect to all other modes; (ii) the total energy of the system is calculated for a set of SiH values around equilibrium, and a sixth-order polynomial fit is used to interpolate these points; (iii) the one-dimensional nuclear Schrodinger equation is solved following the algorithm proposed by Lindberg,[33] which produces the three lowest eigenvalues, E_0, E_1, and E_2, that are then used to compute the first vibrational transitions ω_{01} and ω_{01}, the anharmonicity constant $\omega_e x_e$, and the harmonic stretching frequency ω_e:

$$\omega_{01} = E_1 - E_0$$
$$\omega_{02} = E_2 - E_0$$
$$\omega_e x_e = (2\omega_{01} - \omega_{02})/2$$
$$\omega_e = \omega_{01} + 2\omega_e x_e$$

ω_{01} is is the corrected Si−H stretching frequency to be compared with the fundamental frequency from experiments. The anharmonic frequencies were calculated for the Si−H and C−H stretchings.

The numerical procedure implemented for the vibrational frequencies calculation allows limiting the calculation to an atomic fragment. The first bilayer of silicon atoms together with the different grafting molecules were the atomic fragments employed in the frequency calculations. This approach saves a considerable amount of time and renders virtually the same frequencies as when all the atoms in the unit cell are considered in the frequency calculation.

Results

A value of 2073 cm^{-1} was obtained for the Si−H stretching frequency including anharmonic effects at the PBE/6-21G(d,p) level of theory. This value compares very well the experimental frequency of 2083.7 cm^{-1}.[5] For the harmonic frequency we obtained a stretching of 2111 cm^{-1}. This value compares very well with a recent harmonic frequency calculation performed at an equivalent level of theory (BLYP/6-31G(d,p)) which yielded 2120 cm^{-1} on a slab representing the hydrogenated Si(111)−(1 × 1) surface.[21] For the SiH bending we obtained 627 cm^{-1}, and the experimental value is 626 cm^{-1}.[5]

The changes in the Si−H stretching frequency, computed at the anharmonic level, are shown in Figure 1 as a function of the $-CH_3$, −CCH, and −Cl surface coverage. The absolute values are listed in Table 1. On both the −Cl and −CCH terminated surfaces, ν_s(Si−H) increases with surface coverage,

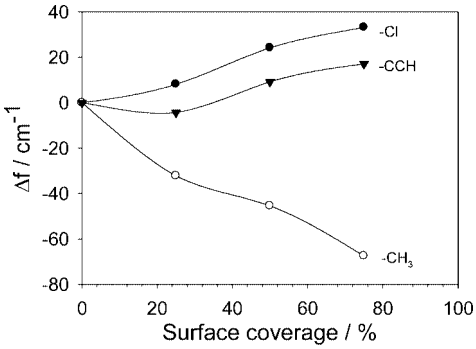

Figure 1. Si−H stretching frequency shift as a function of the surface coverage of −Cl (•), $-CH_3$ (○), and −CCH (▼) groups.

TABLE 1: Si−H Stretching Frequencies (in cm^{-1}) and Si−H Bond Strength *D* (in kcal/mol) as a Function of the Surface Coverage θ of the Grafting Molecule

	−Cl		−CCH		$-CH_3$	
θ	ν_s(Si−H)	D_{Si-H}	ν_s(Si−H)	D_{Si-H}	ν_s(Si−H)	D_{Si-H}
0	2073	81.9	2073	81.9	2073	81.9
25	2081	81.6	2069	81.5	2041	81.4
50	2097	81.8	2082	81.8	2027	81.5
75	2106	81.8	2090	81.9	2005	81.3

TABLE 2: Si−Cl Stretching Frequencies (in cm^{-1}) and Si−Cl Bond Strength *D* (in kcal/mol) as a Function of the Surface Coverage θ

θ	ν_s(Si−Cl)	D_{Si-Cl}
25	516	97.7
50	542	96.7
75	560	95.9
100	577	95.1

whereas on the methylated surface ν_s(Si−H) decreases. Table 1 shows the anharmonic frequencies on each surface together with the corresponding Si−H bond strength. It can be observed that there is no correlation between the frequency changes and the Si−H bond strength, which remains basically constant irrespective of surface coverage or adsorbate type.

Table 2 shows the calculated ν_s(Si−Cl) values as a function of the fraction of surface sites substituted by chlorine atoms. A steady increase in the vibrational frequency is observed as a function of surface coverage. The stretching frequency of 577 cm^{-1} at full coverage is in very good agreement with the experimental value of 586 cm^{-1} reported experimentally.[7] The best estimate of this frequency calculated using a cluster model of the surface at the B3LYP level is 555 cm^{-1}.[34] In another DFT investigation (at the RPBE level with a plane wave basis set) using a slab representation of the surface, a frequency of 561 cm^{-1} was obtained for the Si−Cl stretching mode.[20]

The increase of ν(Si−Cl) with surface coverage is in agreement with experimental results which show that the Si−Cl stretching mode shifts to higher frequencies as a function of the Cl_2 exposure time.[8,35] After 5 min of Cl_2 exposure, a broad and weak Si−Cl band appears first at ∼563 cm^{-1} and then shifts to 584 cm^{-1} at saturation coverage. In the same study,[8] the Si−H stretch band is also observed to shift toward higher frequencies reaching a maximum value of ∼2103 cm^{-1} before disappearance of the band due to complete chlorination of the surface. This value is in very good agreement with the calculated SiH stretching frequency of 2106 cm^{-1} (Table 1) for a chlorine coverage of 75%. At this coverage, every SiH group is surrounded by six SiCl groups.

TABLE 3: Stretching Frequencies (in cm^{-1}) and Si−CCH Bond Strength *D* (in kcal/mol) as a Function of the Surface Coverage θ of −CCH

θ	ν_s(Si−C)	D_{Si-CCH}	ν_s(C′C)	ν_s(C−H)
25	637	119.1	2066	3269
50	646	118.4	2071	3273
75	655	117.6	2077	3276
100	663	116.7	2085	3289

TABLE 4: Asymmetric and Symmetric C−H Stretching Frequency of $-CH_3$ (in cm^{-1}) as a Function of the Surface Coverage θ

θ	ν_a(C−H)	ν_s(C−H)
25	2965	2877
50	2971	2891
75	2973	2896
100	2976	2890

The vibrational frequencies of the acetylated surface are listed in Table 3 as a function of the −CCH surface coverage. The stretching frequencies of the Si−C, C′C, and C−H bonds increase with surface coverage. It can be observed that the ν_s(C′C) values in the range 2066−2085 cm^{-1} overlap with ν_s(Si−H), which are in the range 2069−2090 cm^{-1} (Table 1) on the acetylated surface. These results are in agreement with the experimental observation of a relatively high intensity peak at a frequency of 2080 cm^{-1} which is attributed to the overlap of the peaks originating from the Si−H and C′C vibrations of the partially acetylated Si(111)−H surface.[20] The C′C stretching frequency of 2085 cm^{-1} obtained for the fully covered surface compares very well with the value of 2071 cm^{-1} reported in a previous study performed at the BLYP/6-31G(d,p) level of theory. For the anharmonic frequency of the C−H stretch we obtained a value of 3289 cm^{-1} at full coverage (Table 3), which compares very well with the experimental value of 3300 cm^{-1}.[36]

On the methylated surface we observed a decrease of the Si−H stretching frequency when the methyl surface coverage increases (Table 1). A similar trend has been observed experimentally for both methylated and ethylated surfaces. On the CH_3-terminated Si surface, a small, broad peak centered near 2070 cm^{-1} was observed by transmission infrared spectroscopy.[10] The integrated area of this peak was <10% of the surface coverage of the freshly etched H-terminated Si(111).[10] The same behavior was observed for the ethylated surface for which the 2083 cm^{-1} feature of the hydrogenated surface is broadened and red-shifted to 2070 cm^{-1} after the alkylation process.[7]

Transmission infrared spectroscopy (TIRS) has been used to investigate the surface-bound species formed in the two-step chlorination/alkylation reaction of crystalline (111)-oriented Si surfaces. The CH_3-terminated Si(111) surface exhibited distinct peaks in the C−H stretching region at approximately 2900 cm^{-1}. Peaks at 2909 and 2965 cm^{-1} are attributed[10] to the methyl C−H symmetric and asymmetric stretching vibrations, respectively. In Table 4 we show the variation of ν_s(C−H) and ν_a(C−H) as a function of the $-CH_3$ surface coverage. Both frequencies increase with the surface coverage. At full coverage, we obtained 2890 and 2976 cm^{-1} for the symmetric and asymmetric stretchings, respectively, in good agreement with the experimental values. In an HREELS study of methylated Si(111) obtained by Grignard reaction of photochlorinated Si(111), the asymmetric stretch was observed at 2944 cm^{-1}, respectively, which is in the range of our calculated values.[37]

For the Si−C stretching we did not observe an important frequency variation with the surface coverage of $-CH_3$ groups.

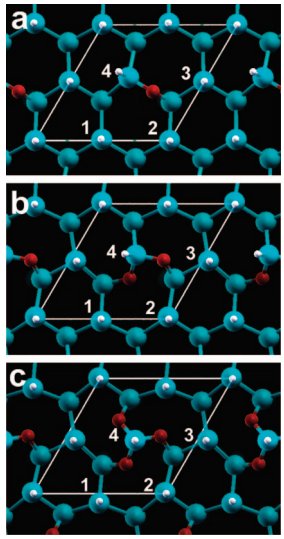

Figure 2. Equilibrium structure of Si(111)−H with (a) one, (b) two, and (c) three silicon back bonds oxidized. Only the first bilayer of silicon atoms is shown. Calculations performed using a (2 × 2) unit cell. The Si−H stretching frequencies of the labeled SiH groups are shown in Table 5.

TABLE 5: Si−H Stretching Frequency (in cm^{-1}) of Each of the Four SiH Groups in the (2 × 2) Unit Cell as a Function of the Number of Oxidized Si−Si Back Bonds[a]

	no. of oxidized Si−Si back bonds		
SiH	1	2	3
1	2069	2058	2055
2	2072	2056	2054
3	2072	2074	2055
4	2074	2102	2213

[a] The back bonds are oxidized for the SiH group labeled 4. See figure 2 for the labeling of the other three SiH groups.

We obtained a frequency of 673 cm^{-1} for 25% surface coverage and a frequency of 670 cm^{-1} at full coverage. The latter value compares very well with the experimental value of 671 cm^{-1} [7].

Oxidized Surfaces. Figure 2 shows the equilibrium structures for the oxidation of one, two, and three silicon back bonds of the hydrogenated surface. The anharmonic Si−H stretching frequency was calculated for each of the four hydrogen atoms in the (2 × 2) unit cell. The results are shown in Table 5. The oxidation of the first back bond has virtually no effect on ν_s(Si−H) as compared to the unoxidized surface. However, the oxidation of the second and third back bonds shifts ν_s(Si−H) to 2102 and 2213 cm^{-1}, respectively. The latter value is close to the experimental value of 2250 cm^{-1} attributed to ν_s(Si−H) with the three back bonds oxidized.[15] The calculated value is 37 cm^{-1} lower that the experimental value. However, we note that in our calculations only one of the four silicon atoms in the (2 × 2) unit cell has been oxidized (see Figure 2c). We expect that further oxidation of the back bonds of the other silicon atoms should increase ν_s(Si−H).

Table 5 also shows that ν_s(Si−H) for the unoxidized silicon atoms is also affected by the oxidation of the neighbor silicon atom. In the case of the trioxidized silicon surface (Figure 2c), ν_s(Si−H) values for the unoxidized silicon atoms decrease to 2054−2055 cm^{-1} from the value of 2073 cm^{-1} obtained for the unoxidized Si(111)−H surface. The dispersion of Si−H stretching values observed in Table 5 for the unoxidized silicon atoms implies that the band associated with the stretching of these SiH groups should broaden during the back-bond oxidation of the other silicon atoms. This is observed experimentally. The sharp absorption peak at 2083 cm^{-1} arising from silicon monohydrides at surface terraces decreases and broadens with immersion time in pure water. This broadening is considered to reflect the progress of very early native oxide growth.[15]

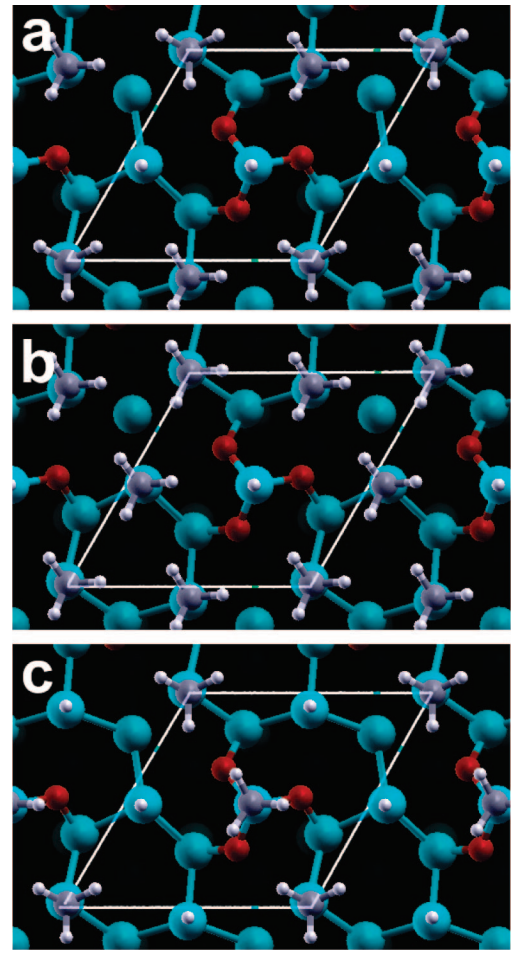

Figure 3. Equilibrium structures of partially oxidized and methylated silicon surfaces: (a) trioxidized SiH group with a 50% surface coverage of methyl groups, (b) trioxidized SiH group with a 75% surface coverage of methyl groups, and (c) trioxidized methylated silicon atom with 50% surface coverage of methyl gropus.

TABLE 6: Si−H Stretching Frequency (in cm^{-1}) of a Trioxidized SiH Group as a Function of the Surface Coverage of Methyl Groups[a]

θ	ν_s(O_3Si−H)
0	2213
50	2183
75	2169

[a] Figures 3a and 3b correspond to θ = 50% and 75%, respectively.

We also investigated the effect of alkylation of the hydrogenated silicon atoms surrounding the O_3Si−H moiety on the Si−H stretching frequency of O_3Si−H. The equilibrium structures for 50% and 75% coverage of CH_3 are shown in Figures 3a and 3b. Table 6 lists ν_s(O_3Si−H) as a function of the methyl coverage. As in the case of the unoxidized surface, ν_s(O_3Si−H) decreases as the surface coverage increases.

Figure 3c shows the equilibrium structure for a 50% coverage of methyl groups in which one-half of the methylated silicon atoms have the three back bonds oxidized. The stretching frequencies of the two unoxidized SiH groups are 2019 and

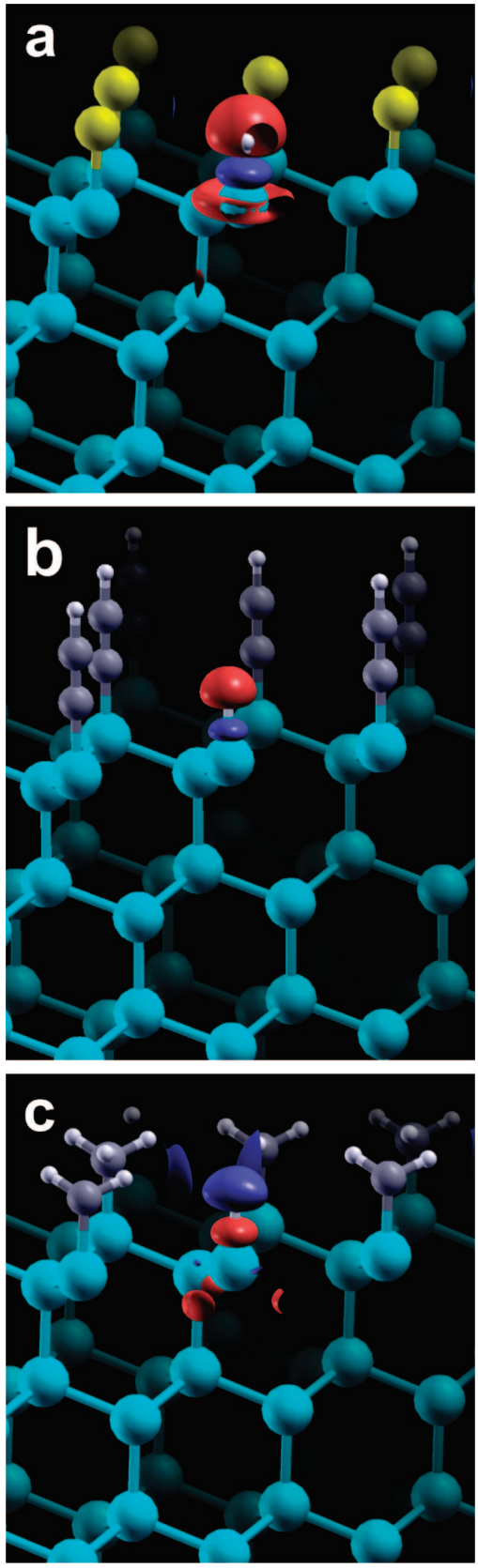

Figure 4. Electron density difference around the SiH group for surfaces grafted with a 75% surface coverage of (a) −Cl, (b) −CCH, and (c) $-CH_3$ groups. The electron density difference was computed by subtracting the electron density of the hydrogenated surface from the density of the grafted surface. The red contour corresponds to depletion of electron density, and the blue contour corresponds to accumulation. Isocontour: ±0.0005 electron $bohr^{-3}$.

2024 cm^{-1}, which are slightly lower than on the unoxidized surface (2027 cm^{-1}, Table 1). The oxidation of the methylated silicon atom has a small effect on the C−H stretching of the methyl group: ν_s(C−H) increases from 2890 cm^{-1} (unoxidized surface) to 2898 cm^{-1} (oxidized surface). In the case of the asymmetric stretching mode, ν_a(C−H) increases from 2976 cm^{-1} (unoxidized surface) to 2990 cm^{-1} (oxidized surface). These values compare very well with the stretching peaks at 2904 and 2963 cm^{-1} obtained for the symmetric and asymmetric modes of CH_3 on an oxidized silicon surface functionalized with methyl groups.[38]

Discussion

The variations of ν_s(Si−H) observed on the different grafted surfaces (Figure 1) indicate that the adsorbate modifies the electronic structure of the SiH group. A decrease of ν_s(Si−H) with the increase in the surface coverage of the grafting molecule can be rationalized on the basis of a reduced dynamic coupling among SiH oscillators due to the elimination of the dipole−dipole interactions. This effect could be attributed to the decrease of ν_s(Si−H) on the methylated surface, but it cannot explain the increase of ν_s(Si−H) on the chlorinated and acetylated surfaces. Besides, the dynamic dipole coupling only accounts for a few cm^{-1},[3,4] whereas the changes observed in Figure 1 are several tens of cm^{-1}.

The increase of ν(Si−H) on the Si−Cl modified surface has its parallel on the Si−I surface.[39] It has been reported that after immersion of the atomically flat H-terminated Si(111) in a HI + I_2 solution, the sharp peak at 2083.7 cm^{-1} disappears nearly completely, accompanied by the appearance of new broad bands at around 2095 cm^{-1}. These bands have been assigned to remaining terrace SiH groups with the vibrational energies modified by neighboring Si−I bonds.[39]

In order to understand how neighboring Si−Cl, Si−CH_3, and Si−CCH bonds affect the electronic structure of the SiH group, we investigated the electron density and the projected density of states (DOS) around the SiH group. Figure 4 shows a contour plot of the electron density difference around the SiH group. The difference was calculated by subtracting the density of the hydrogenated surface to the density of the grafted surface. In all cases, the grafted surfaces had an adsorbate surface coverage of 75%, which implies that each SiH group is surrounded by a hexagon of six Si−Cl, Si−CCH, or Si−CH_3 groups. On the chlorinated and acetylated surfaces, there is an increase of electron density along the Si−H bond which correlates with the increase of the stretching frequency of the SiH group. The charge accumulation along the Si−H bond is more pronounced for the chlorinated surface for which the frequency shift is also more pronounced (Figure 1). On the methylated surface, the electron density decreases along the Si−H bond which correlates with the decrease of its vibrational frequency.

The electron density difference was integrated over the x and y coordinates to obtain $\Delta\rho(z)$, the density difference in the direction perpendicular to the surface. Figure 5 clearly shows the polarization of the electron density around the SiH bond induced by the different adsorbates. On the Si−Cl and Si−CCH modified surfaces, a peak of accumulation of electron density can be observed along the SiH bond at the expense of the electron density around the Si and H atoms. The reverse trend is observed for the CH_3 modified surface.

The area under the peak of accumulation or depletion of electron density along the Si−H bond was integrated for the different adsorbates and surface coverages. Figure 6 shows the frequency shift as a function of the charge thus calculated. It

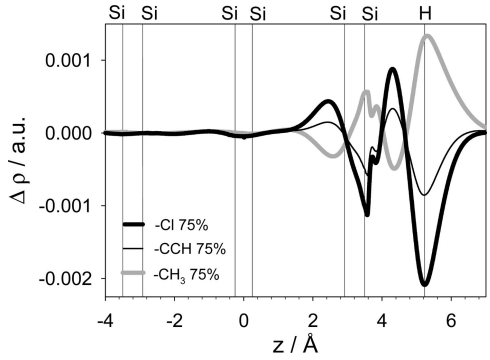

Figure 5. Electron density difference around the SiH group in the direction perpendicular to the surface. The vertical lines indicate the planes containing the silicon as well as the H atoms of the SiH group.

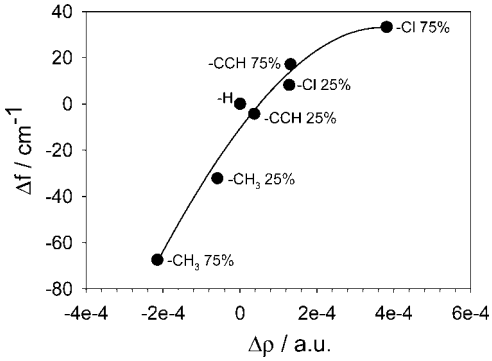

Figure 6. Stretching Si−H frequency shifts as function of the accumulation or depletion of electron charge along the Si−H bond for different surface coverages of the grafting molecules' surfaces.

can be observed that for all adsorbates and surface coverages, the positive frequency shifts are associated with an accumulation of electron density along the Si−H bond whereas the negative frequency shifts correspond to a depletion of electron density.

Figure 7a shows the density of states projected on the atomic orbitals of the SiH group for the fully hydrogenated surface. In the energy range between 0.0 and −4.5 eV, the resonances between the peaks of the H(1s) and Si($3p_z$) DOS can be appreciated. These resonances correspond to the σ bonding orbital between the Si and H atoms. The Si(3s) states have a low density in the range from −4.5 to 0.0 eV, and their density increases at lower energies. The Si(3s) states at lower energies are involved in the Si−Si bonding. The Si($3p_x$) and Si($3p_y$) DOS are degenerate, and they are involved in the bonding of the silicon atom of the SiH group with the surrounding silicon atoms.

Figures 7b-d show the projected DOS for the $-CH_3$, −Cl, and −CCH modified surfaces with a 75% surface coverage. For these grafted surfaces, the DOS shifts toward lower energies as compared to the hydrogenated silicon surface. The prominent peak at −3.9 eV in the DOS of the hydrogenated surface shifts to −4.6 and −4.4 eV for the methylated and acetylated surfaces, respectively. In the case of the chlorinated surface, a splitting is observed with peaks at −3.7 and −4.3 eV. The charge density associated with these peaks is shown in Figure 8. It can be observed that the crystalline orbitals are delocalized around the SiH groups as well as around the SiCl, $SiCH_3$, and SiCCH groups. Therefore, it becomes clear that the different grafting groups will affect the electronic structure of the SiH group.

At energies lower than −6 eV, the density of the Si(3s) states increases and is different for the different surfaces. For the −CCH modified surface, for example, a pronounced peak is

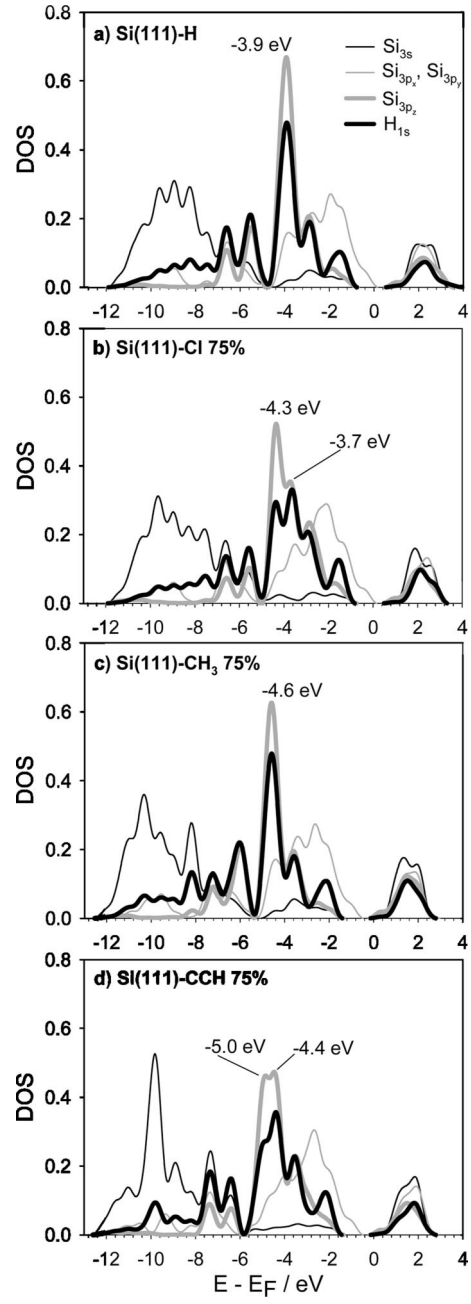

Figure 7. Density of states projected on the Si(3s), Si(3p), and H(1s) orbitals of the SiH group for (a) the hydrogenated surface and the grafted surfaces with a 75% surface coverage of (b) −Cl, (c) $-CH_3$, and (d) −CCH. The energies are relative to the Fermi energy of each surface.

observed at −10 eV (Figure 7d). The states in this energy range are delocalized over the silicon lattice. This implies that the adsorbates not only modify the electronic structure of the SiH group, but also modify the states involved in the bonding of the Si atom of the SiH group with the other silicon atoms.

The area under the H(1s) and Si($3p_z$) DOS was integrated in the energy range in which these two states show the resonances arising from the σ bonding between these two atoms. Figure 9 shows the stretching SiH frequency shifts for the different grafted surfaces as a function of the integrated DOS. It can be observed that the changes in the stretching frequency correlate with the changes in the density of states.

Even in the absence of the silicon surface, the polarization of the electron density of the SiH group by the different

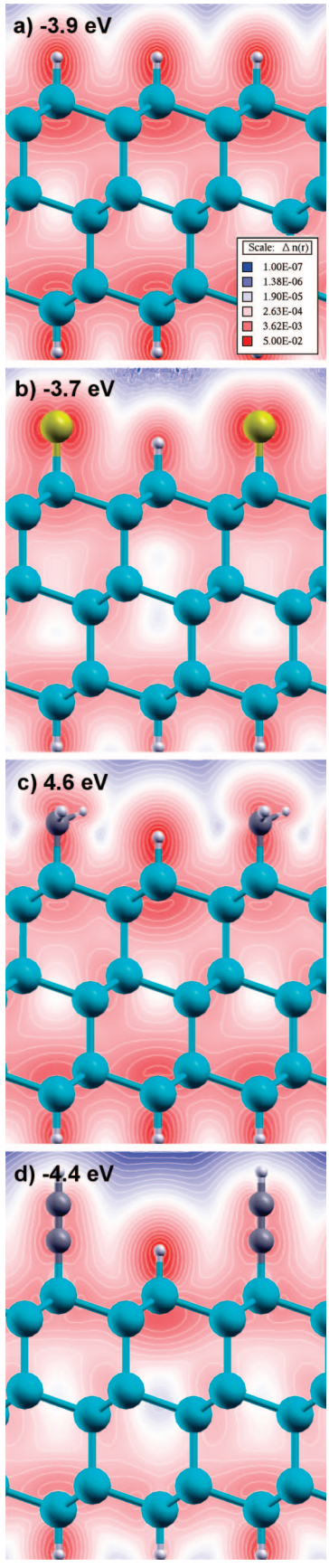

Figure 8. Charge density distribution of the states corresponding to the main peaks of the DOS shown in Figure 7. The peak energy is shown in the insets: (a) hydrogenated, (b) chlorinated, (c) methylated, and (d) acetylated surface. The surface coverage of the grafted surfaces is 75%.

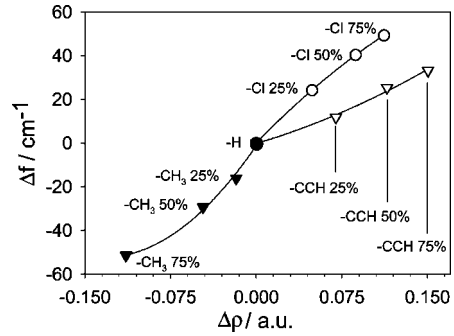

Figure 9. Stretching SiH frequency shifts as function of the integrated H(1s) and Si($3p_z$) DOS.

adsorbates can explain the trends in the observed frequency shifts. We performed a calculation for an array of H_3Si-H molecules surrounded by six H_3Si-R molecules, where $-R$ is $-Cl$, $-CH_3$, and $-CCH$ (Figure 10). The unit cell was the same as on the silicon surface. For $-Cl$ and $-CCH$ we obtained an increase in the SiH stretching frequency of 31 and 9 cm^{-1}, whereas for the $-CH_3$ group we obtained a decrease of -38 cm^{-1} in ν_s(SiH). The corresponding frequency shifts on the silicon surface are 33, 17, and -67 cm^{-1} for the $-Cl$, $-CCH$, and $-CH_3$ grafted surfaces (see Figure 1, 75% coverage). The difference between the frequency shifts of both calculations is a measure of the contribution of the surface. In the case of the $-Cl$ group, virtually all the frequency shift can be obtained from the array of H_3Si-Cl molecules.

In order to further evaluate the effect of the surrounding molecules on the stretching frequency, we calculated the stretching Si−Cl frequency for a slab of H_3Si-Cl molecules as a function of the intermolecular spacing. For each spacing, the geometry of the H_3Si- fragment was kept fixed whereas the Si−Cl distance was optimized and then ν_s(SiCl) was calculated. Figure 11 shows that ν_s(SiCl) varies from 531 cm^{-1} at long separations up to 566 cm^{-1} at an intermolecular spacing of 3.87 Å (the DFT equilibrium spacing of SiCl groups on the 111 surface). This value is very close to the Si−Cl stretching frequency of 577 cm^{-1} obtained on the fully chlorinated surface (Table 3). This shows that even in the absence of the surface, most of the Si−Cl vibrational frequency can be recovered provided that the intermolecular spacing of the oscillators is the same as on the grafted surface. As shown in Figure 12, the stretching Si−Cl frequency shows a linear correlation with the Si−Cl bond distance which decreases as the intermolecular separation decreases.

An equivalent calculation as that shown in Figure 11, but using a slab of H_3Si-H molecules, also shows an increase in the Si−H stretching frequency as the intermolecular separation decreases. However, the change is only 7 cm^{-1}. This frequency shift is in the expected range for the coupling of SiH oscillators.[3,4] Therefore, the large variations in ν_s(Si−H) shown in Figure 1 for the different grafted surfaces cannot be attributed to the coupling or decoupling of SiH oscillators.

On the alkylated surfaces, the IR band associated with the unsubstituted Si−H bonds is always broadened.[7,10] Our results showed that the influence of the local environment (the nature of the attached molecules and their surface coverage) has an important influence on the Si−H stretching vibration. Another degree of freedom results from the fact that for a given substitution percentage, a variety of substitution patterns exist. For example, for a substitution of 50%, the zigzag-type pattern is more stable than the linear pattern.[40] However, the energy difference between the different patterns is only a few kilo-

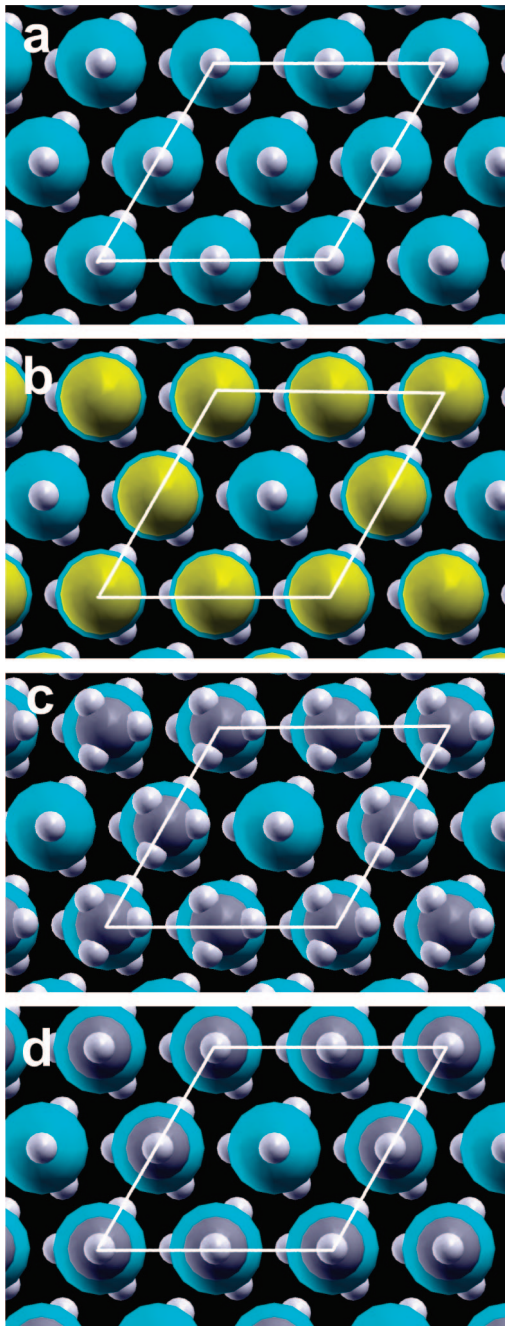

Figure 10. Equilibrium structures of molecular slabs of (a) H_3SiH, (b) H_3SiH + H_3Si-Cl, (c) H_3SiH + H_3Si-CH_3, and (d) H_3SiH + $H_3Si-CCH$. The unit cell parameter is the same as on the Si(111) surface.

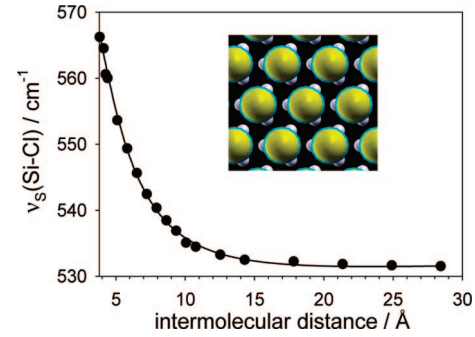

Figure 11. Variation of Si−Cl stretching frequency as a function of the intermolecular separation for a slab of H_3Si-Cl molecules (inset).

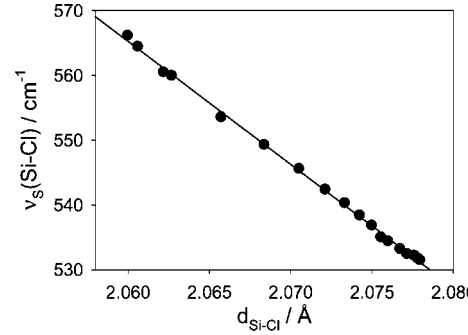

Figure 12. Correlation between Si−Cl stretching frequency and Si−Cl bond length as a function of the intermolecular separation of H_3Si-Cl molecules.

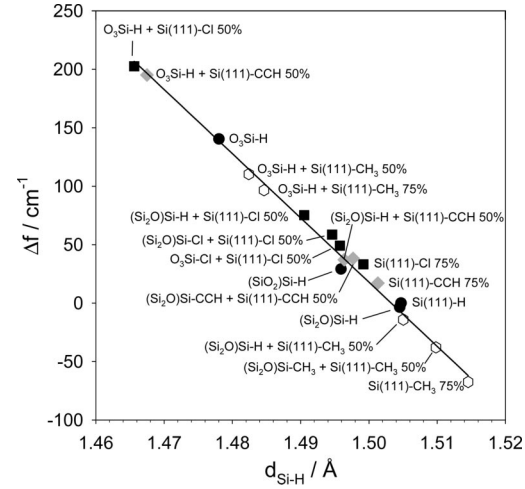

Figure 13. Correlation between Si−H stretching frequency and Si−H bond length for all the grafted and oxidized surfaces investigated. The calculations were performed with a (2 × 2) unit cell. The labels indicate the surface coverage of the grafting molecule as well as the extent of subsurface oxidation.

calories per mole. It has been pointed out that several of the highly ordered patterns are simultaneously present as relatively small patches on the surface. As a result, disordered patterns will be present at the boundaries between ordered domains.[40] We therefore think that the dispersion of the Si−H stretching frequencies for monolayers with a surface coverage close to 50% reveals the large variety of local environments of the unsubstituted SiH groups.

Figure 13 shows a plot of ν_s(SiH) as a function of the Si−H bond length for all the systems investigated in this work. It can be observed that the correlation between both quantities is very good. The most positive frequency shifts are observed for partially oxidized and chlorinated silicon surfaces. We attribute the changes in the SiH bond length to the polarization of the electron density around the SiH group induced by the different adsorbates as well as by subsurface oxygen atoms. This is effectively confirmed when the SiH bond is polarized with an electric field perpendicular to the surface. Figure 14 shows a plot of ν_s(SiH) as a function of the Si−H bond length optimized for different electric fields. It can be observed that there is a linear correlation in the electric field range considered.

The linear correlation between bond distance and vibrational frequency was discovered long ago by Badger and is known as Badger's rule.[41] It is applicable to a wide range of compounds. The C−H frequencies of n-alkanes, for example, were found to correlate linearly with calculated ab initio bond lengths with

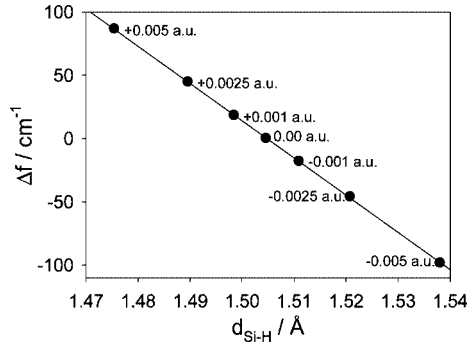

Figure 14. Si−H stretching frequency vs Si−H bond length for different electric fields perpendicularly applied to the Si(111)−H surface.

very high precision.[42a] Molecules containing SiH[42b,c] as well as GeH[42c] bonds also show a linear correlation between the vibrational frequency and the equilibrium bond length. Our results indicate that Badger's rule for the SiH bond is also observed on the Si(111) surface.

We did not find any correlation between the changes in ν_s(SiH) and the SiH bond energy on the unoxidized surfaces. Table 1 shows that irrespective of surface coverage or adsorbate type, the SiH bond energy remains virtually constant. Tables 2 and 3 shows that the Si−Cl and Si−C bond energies for the −Cl and −CCH grafted surfaces decrease with the increase in surface coverage. In a previous paper[43] we showed that this decrease is due to a weakening of the surface bond as well as to repulsive interactions among the adsorbates. Therefore, the increase in the stretching frequencies shown in Tables 2 and 3 is not related to a strengthening of the surface bonding, as the reverse trend is observed with the increase in surface coverage.

Conclusions

The vibrational frequencies of the hydrogenated Si(111) surface grafted with −Cl, $-CH_3$, and −CCH groups were computed at the PBE/6-21G(d,p) level of theory considering anharmonic effects for the Si−H and C−H vibrations. The calculated frequencies show very good agreement with the experimental values. For the Si−H stretching and bending frequencies, we obtained 2073 and 627 cm^{-1}. On the grafted surfaces with a 100% surface coverage we obtained the following: ν_s(SiCl) = 577 cm^{-1} for the chlorinated surface; ν_s(Si−C) = 670 cm^{-1}, ν_s(C−H) = 2890 cm^{-1}, and ν_a(C−H) = 2976 cm^{-1} for the methylated surface; and ν_s(Si−C) = 663 cm^{-1}, ν_s(C−C) = 2085 cm^{-1}, and ν_s(C−H) = 3289 cm^{-1} for the acetylated surface.

The SiH vibrational frequency is very sensitive to the surface coverage of the grafting group. The adsorbates polarize the electron density around the SiH group leading to accumulation or depletion of electron density along the Si−H bond. The Si−H stretching frequency increases with the surface coverage of −CCH and −Cl species, and it decreases with the increase in the surface coverage of $-CH_3$. Increased frequencies correlate with charge accumulation along the Si−H bond and vice versa. The effect of the polarization of the electron density of the SiH group on its vibrational frequency could also be simulated qualitatively by applying electric fields perpendicular to the surface. Even in the absence of the surface, a periodic array of H_3Si−H molecules embedded in H_3Si−R molecules (R = $-CH_3$, −Cl, and −CCH) can reproduce the trends in ν_s(Si−H). The polarization of the electron density also influences the Si−H bond length. Therefore, a very good correlation was observed between frequency shifts and SiH bond length.

On the oxidized surface ν_s(Si−H) increases with the number of Si−Si back bonds oxidized whereas ν_s(Si−H) decreases for the unoxidized SiH groups. A value of 2213 cm^{-1} was obtained for the stretching frequency of a SiH group with its three back bonds oxidized in a (2 × 2) unit cell in which the remaining three SiH groups were unoxidized.

Acknowledgment. Financial support from FONCyT (Grant PICT 2005-32893), CONICET (Grant PIP 5903), and SECYT-UNC is gratefully acknowledged. M.F.J. thanks CONICET for the fellowships granted.

References and Notes

(1) Chabal, Y. J.; Harris, A. L.; Raghavachari, K.; Tully, J. C. *Int. J. Mod. Phys. B* **1993**, *7*, 1031.
(2) Weldon, M. K.; Marsico, V. E.; Chabal, Y. J.; Hamann, D. R.; Christman, S. B.; Chaban, E. E. *Surf. Sci.* **1996**, *368*, 163.
(3) Newton, T. A.; Boiani, J. A.; Hines, M. A. *Surf. Sci.* **1999**, *430*, 67.
(4) Jakob, P.; Chabal, Y. J.; Raghavachari, K. *Chem. Phys. Lett.* **1991**, *187*, 325.
(5) Higashi, G. S.; Chabal, Y. J.; Trucks, G. W.; Raghavachari, K. *Appl. Phys. Lett.* **1990**, *56*, 656.
(6) Faggin, M. F.; Green, S. K.; Clark, I. T.; Queeney, K. T.; Hines, M. A. *J. Am. Chem. Soc.* **2006**, *128*, 11455.
(7) Rivillon, S.; Michalak, D. J.; Chabal, Y. J.; Wielunski, L.; Hurley, P. T.; Lewis, N. S. *J. Phys. Chem. C* **2007**, *111*, 13053.
(8) Rivillon, S.; Amy, F.; Frank, M.; Chabal, Y. J. *Appl. Phys. Lett.* **2004**, *85*, 2583.
(9) Rivillon, S.; Chabal, Y. J.; Webb, L. J.; Michalak, D. J.; Lewis, N. S.; Halls, M. D.; Raghavachari, K. *J. Vac. Sci. Technol.* **2005**, *A23*, 1100.
(10) Webb, L. J.; Rivillon, S.; Michalak, D. J.; Chabal, Y. J.; Lewis, N. S. *J. Phys. Chem. B* **2006**, *110*, 7349–7356.
(11) Niwano, M.; Kageyama, J.; Kurita, K.; Kinashi, K.; Takahashi, I.; Miyamoto, N. *J. Appl. Phys.* **1994**, *76*, 2157.
(12) Miura, T.; Niwano, M.; Shoji, D.; Miyamoto, N. *J. Appl. Phys.* **1996**, *79*, 4373.
(13) Neuwald, U.; Feltz, A.; Memmert, U.; Behm, R. J. *J. Appl. Phys.* **1995**, *78*, 4131.
(14) Sugita, Y.; Watanabe, S. *Mater. Res. Soc. Symp. Proc.* **1997**, *448*, 63.
(15) Ogawa, H.; Ishikawa, K.; Inomata, C.; Fujimura, S. *J. Appl. Phys.* **1996**, *79*, 472.
(16) Niwano, M. *Surf. Sci.* **1999**, *427*, 199.
(17) Halls, M. D.; Raghavachari, K. *J. Phys. Chem. B* **2004**, *108*, 19388.
(18) Queeney, K. T.; Chabal, Y. J.; Raghavachari, K. *Phys. Rev. Lett.* **2001**, *86*, 1046.
(19) Halls, M. D.; Raghavachari, K. *J. Phys. Chem. B* **2004**, *108*, 19388.
(20) Nishiyama, K.; Tanaka, Y.; Harada, H.; Yamada, T.; Niwa, D.; Inoue, T.; Homma, T.; Osaka, T.; Taniguchi, I. *Surf. Sci.* **2006**, *600*, 1965.
(21) Ferguson, G. A.; Raghavachari, K.; Michalak, D. J.; Chabal, Y. *J. Phys. Chem. C* **2008**, *112*, 1034.
(22) Ferguson, G. A.; Raghavachari, K. *J. Chem. Phys.* **2006**, *125*, 154708.
(23) Gai, H.; Voth, G. A. *J. Chem. Phys.* **1994**, *101*, 1734.
(24) Sun, Y.; Gai, H.; Voth, G. A. *Chem. Phys.* **1996**, *205*, 11.
(25) Dovesi, R.; Causa, M.; Angonoa, G. *Phys. Rev. B* **1981**, *24*, 4177.
(26) Torres, F. J.; Civalleri, B.; Pisani, C.; Ugliengo, P. *J. Phys. Chem. B* **2006**, *110*, 10467.
(27) Perdew, J. P.; Burke, K.; Ernzerhof, M. *Phys. Rev. Lett.* **1996**, *77*, 3865.
(28) (a) Broyden, C. G. *J. Inst. Math Appl.* **1970**, *6*, 76. (b) Fletcher, R. *Comp. J.* **1970**, *13*, 317. (c) Goldfarb, D. *Math. Comput.* **1970**, *24*, 23. (d) Shanno, D. F. *Math. Comput.* **1970**, *24*, 647.
(29) Pascale, F.; Zicovich-Wilson, C. M.; Gejo, F. L.; Civalleri, B.; Orlando, R.; Dovesi, R. *J. Comput. Chem.* **2004**, *25*, 888.
(30) Merawa, M.; Labeguerie, P.; Ugliengo, P.; Doll, K.; Dovesi, R. *Chem. Phys. Lett.* **2004**, *387*, 453.
(31) Pascale, F.; Tosoni, S.; Zicovich-Wilson, C.; Ugliengo, P.; Orlando, R.; Dovesi, R. *Chem. Phys. Lett.* **2004**, *396*, 308.
(32) Merawa, M.; Civalleri, B.; Ugliengo, P.; Noel, Y.; Lichanot, A. *J. Chem. Phys.* **2003**, *119*, 1045.
(33) Lindberg, B. *J. Chem. Phys.* **1988**, *88*, 3805.

(34) Ricca, A.; Musgrave, C. B. *Surf. Sci.* **1999**, *430*, 116.
(35) Gao, Q.; Cheng, C. C.; Chen, P. J.; Choyke, W. J.; Yates, J. T., Jr. *J. Chem. Phys.* **1993**, *98*, 8308.
(36) Yamada, T.; Shirasaka, K.; Noto, M.; Kato, H. S.; Kawai, M. *J. Phys. Chem. B* **2006**, *110*, 7357.
(37) Yamada, T.; Kawai, M.; Wawro, A.; Suto, S.; Kasuya, A. *J. Chem. Phys.* **2004**, *121*, 10660.
(38) Schmohl, A.; Khan, A.; Hess, P. *Superlattices Microstruct.* **2004**, *36*, 113.
(39) Zhou, X.; Ishida, M.; Imanishi, A.; Nakato, Y. *J. Phys. Chem. B* **2001**, *105*, 156.
(40) Sieval, A. B.; van den Hout, B.; Zuilhof, H.; Sudholter, E. J. R. *Langmuir* **2001**, *17*, 2172–2181.
(41) Badger, R. M. *J. Chem. Phys.* **1934**, *2*, 128.
(42) (a) Aljibury, A. L.; Snyder, R. G.; Strauss, H. L.; Raghavachari, K. *J. Chem. Phys.* **1986**, *84*, 6872. (b) McKean, D. C.; Torto, I.; Boggs, J. E.; Fan, K. *J. Mol. Struct. THEOCHEM* **1992**, *260*, 27. (c) McKean, D. C. *J. Mol. Struct.* **1984**, *113*, 251.
(43) Juarez, M. F.; Soria, F. A.; Patrito, E. M.; Paredes-Olivera, P. *J. Phys. Chem. C* **2008**, *112*, 14867.

JP808104F